A three-dimensional phase-field simulation of pulsed laser induced epitaxial growth of silicon

MOHAMMAD REZA TAJARI MOFRAD[*], ANTONIO LA MAGNA[a],
RYOICHI ISHIHARA, HE MING, KEES BEENAKKER

*University of Technology, Delft Institute of Microelectronics and Submicrontechnology (DIMES),
Laboratory of Electronic Components, Technology and Materials (ECTM),
P.O. box 5053, 2600 GB Delft, The Netherlands
[a]CNR-IMM Sezione Catania, Stradale Primosole 50, I-95121 Catania, Italy*

The aim of this work is to understand the mechanism behind facet formation during epitaxial growth of silicon induced by excimer laser which leads to formation of subgrains in the final crystallized films. We use a phase-field methodology applied to a three-dimensional finite elements simulation of the melt and regrowth phase of silicon during the excimer laser annealing. Due to the specific patterning of the structure, a thermal gradient exists which leads to geometrically non-uniform solidification front. This observation may be the main reason for the generation of subgrains.

1. Introduction

Downscaling the transistor dimensions have been a successful approach for increasing the density and performance of the integrated circuits for decades. Short-channel effects and critical gate dielectric requirements, however, cause serious difficulties in recent aggressive downscaling. To be able to satisfy Moore's predictions, several approaches have been introduced. Among them three-dimensional stacking of electronic circuits offers the best perspective. The three-dimensional Integrated Circuits (3D ICs) offer higher chip density without any size reduction of transistors while shorter interconnects between critical modules of the chip which will lead to less power dissipation and higher speed. Among different 3D IC technologies, monolithic stacking offers the most freedom in design and together with that the most amount of the named advantages.

To be able to make monolithic stacking a serious candidate for the industry, some technological issues need to be solved. Obtaining high quality silicon films have been an issue for decades [1]. 2D location controlled large silicon grains have been obtained using excimer laser annealing (ELA) methods which have led to high mobility thin film transistors (TFTs)[2][3]. These single-grain TFTs are the perfect candidate for the stacking as they can be made using low temperatures. However, the location controlled grains have random crystallographic orientations which cause variations in electrical behavior of the transistors, unless the orientation of the seed is controlled. One approach overcoming the orientation control in the crystallized film is laser induced epitaxial process. This process contains melting a layer of amorphous silicon (a-Si), which is in contact with a seeding layer crystalline silicon (c-Si). Solidification starts from the interface of the molten Si and c-Si by which the solidified silicon inherits the orientation of the c-Si. Unfortunately, the epitaxially grown silicon is not perfect. It has been found that twin grain boundaries are generated at the SiO_2 window [4]. Our aim of this study is to understand, by means of simulation, the mechanism behind the defects formation.

Since the interface between the liquid and solid silicon seems to be related to the defect formation during vertical growth, phase-field methodology has been utilized to track the interface in order to find a relation between the phase, temperature, thermal stress and origin of defects. Specific patterning of the structures demands a 3D simulation in order to obtain the correct results taking into account the effects of curvature on supercooling and solidification.

2. Experiment

The aim of the experiment is to obtain c-Si by melting the a-Si by means of ELA and inherit the crystallographic orientation of the seeding layer. The starting material is a 250 nm thick c-Si on oxide on bulk silicon. We deposit 500 nm thick SiO_2 using plasma enhanced chemical vapor deposition (PECVD) with tetra-ethyl-ortho-silicate (TEOS) precursor and pattern the layer in arrays of 1 µm deep holes. Subsequent deposition and dry etching of a 500 nm thick layer of PECVD SiO_2 results in holes having a diameter of approximately 200 nm. We deposit a 250 nm thick a-Si on top of this structure using low-pressure chemical vapor deposition (LPCVD) at 545 °C. Fig. 1 shows the schematics of the final structure.

1. a-Si (250 nm)
2. Oxide (500 nm)
3. c-Si (seed) (250 nm)
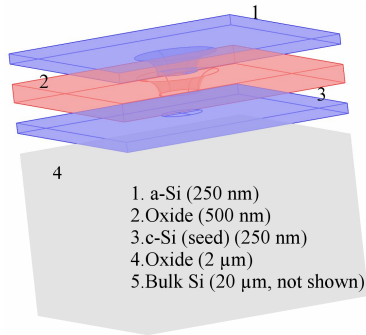4. Oxide (2 μm)
5. Bulk Si (20 μm, not shown)

Fig. 1. This figure shows the schematics of the laser induced epitaxy process. There is an artificial distance placed between the layers to give more clarity.

By ELA we melt the a-Si on the surface and in the holes down to the interface of a-Si and c-Si. C-Si acts a the heat sink at thus the solidification starts from c-Si. At this point, there exists no a-Si in the structure, only molten Si on top of c-Si. The molten Si inherits the orientation of the seeding c-Si during solidification. This is confirmed by EBSD measurements of the crystallized films. Fig. 2 shows the inverse pole figure map, image quality map overlaid with grain boundary component map and pole figure of the surface of a crystallized Si film with <100>-oriented c-Si as seed. We can observe that the crystallized film also shows strong <100> surface orientation. This is the proof of a successful epitaxial growth.
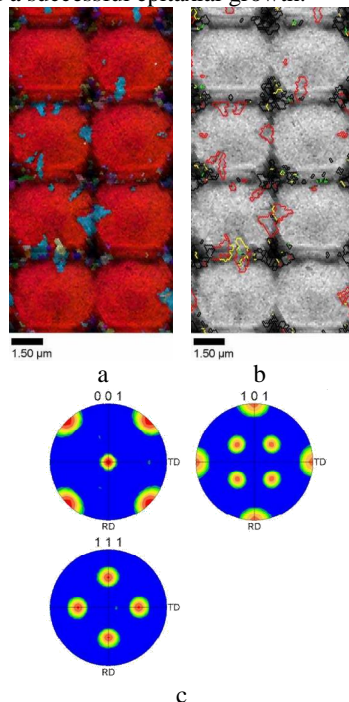

Fig. 2. Inverse pole figure (IPF) map (a), image quality map overlaid with grain boundary component map (b) and pole figure (c) of the grains from (100) oriented seed with laser fluence at 1400 mJ/cm² and with substrate heating up to 450 ℃. Coincidence Site Lattice (CSL) boundaries are colored as follows: Σ3 red; Σ9 yellow; Σ27 blue. The CSL boundaries inside the islands are mainly Σ3.

A reproducible presence of subgrains at fixed locations around the seeding hole is observed. TEM analysis of the cross-section of the seeding holes shows formation of facets at the SiO_2 sidewall. The angle of the SiO_2, solid and molten silicon is the main parameter that induces the formation of facets [5]. This is the main motivation for setting up a simulation tool to be able to test the different process parameters for reduction of the subgrain formation. Figure 3 shows the cross-sectional TEM images of grains grown from <100>-orientated seed. Vertical and lateral growth are visible. Part (b) is the surface TEM picture showing the four secondary subgrains inside one large grain.

2.1 Phase-Field Method

Phase-field methodology offers solution to the free boundary problems introduced by the melting and solidification of films after ELA. The main advantage of this methodology is that the position of the interface between two different phases is known as a variable called phase (Ψ). This variable has finite width and couples the macroscopic parameters like thermal parameters to microscopic ones like surface tension and diffusivity.
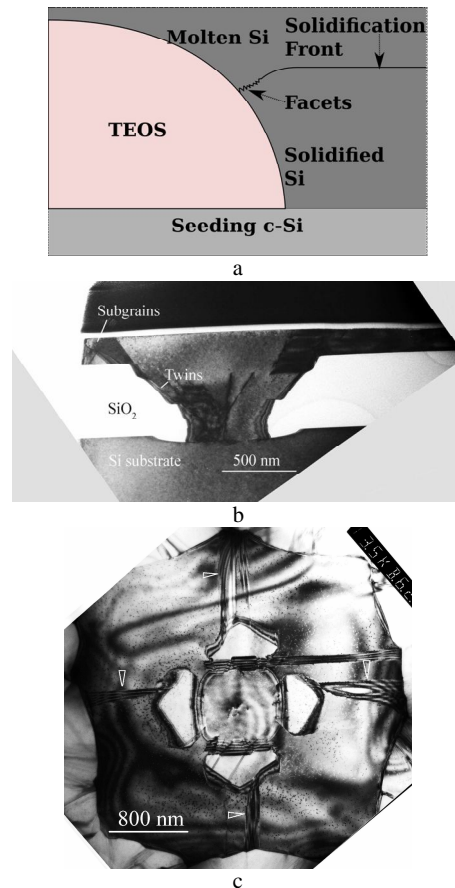

Fig. 3. Schematics of facet formation during the vertical growth (a), cross-sectional TEM image of grains grown from <100>-orientated seed showing epitaxial growth from the seed (b) and surface TEM showing four secondary subgrains inside one large grain (c).

The dynamics of phase transitions can be modeled using two partial differential equations (PDEs) which are coupled together by coupling equations. There exist different methods for choosing the coupling equations. We chose the method explained in [6] due to it's advantage in convergence.

The basic phase-field equations are as follows:

$$\tau \partial_t \Psi = W^2 \nabla^2 \Psi - \frac{F(\Psi, \lambda u)}{\partial \Psi}$$

$$\partial_t u = D \nabla^2 u + \partial_t h(\Psi)/2$$

where $u \equiv (T - T_M)/(L/c_p)$ is the dimensionless temperature field, in which T is the absolute temperature, L is the latent heat which is released during silicon's phase from solid to liquid and c_p is the specific heat capacity which is a measure for the energy needed to raise the temperature of silicon. Furthermore, W is the interface thickness between the solid and liquid phase, τ is a measure for surface relaxation time and λ controls the coupling between phase and diffusion field. λ contains thermal conductivity (K) of the materials to gather with 3 fitting parameters. F is a function of Ψ and λu, which can be separated in two functions of f and g as follows:

$$F(\Psi, \lambda u) = f(\Psi) + \lambda g(\Psi) u$$

$$g(\Psi) = b/2h(\Psi)$$

where b is a normalization factor obtained from the values of $h(\Psi)$ at solid and liquid state (+1 and -1). In this way the coupling between the heat diffusion equation and phase equation is set.
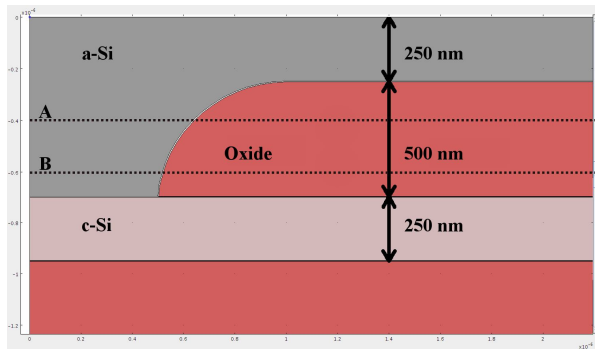

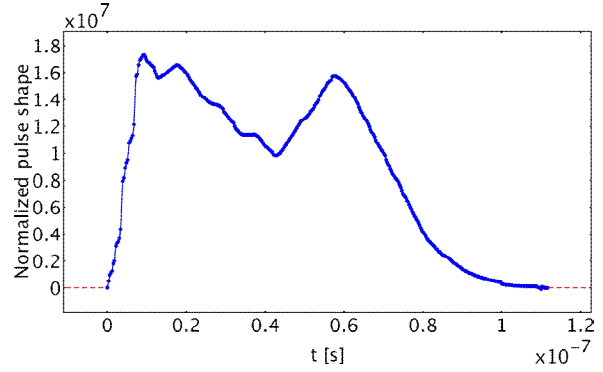Fig. 4. The 2D cross section of the simulation structure.

Fig. 5. The normalized pulse shape used in the simulation consists of two pulses, 25 ns long each, with 40 ns pulse delay.

In practice, we have a three phase system: amorphous, crystalline and liquid. To optimize the simulation time, we remove of the amorphous phase by introducing a flag which changes the properties of amorphous domain permanently once melting has occurred. In this way we can reduce one PDE which results into faster simulation.

3. Results and discussion

The 2D cross-section of the simulation structure is shown in Fig. 4. ELA consists of two 25 ns long pulses with the FWHM of XeCl shown in Figure 5, overlapping to make 70 ns pulse shape. A total amount of 1.4 J/cm^2 is transfered in to the system. During the laser processing, the substrate is heated up to 450 °C using a heater. Most of this energy is absorbed in the first few nanometers of a-Si. A-Si melts down reaching the c-Si. Maximum melt depth using this condition is 800 nm, reached at t=124 ns. To compare the simulation results with the experimental ones, the graphs in Fig. 6 are produced. To understand the onset of melt, multiple simulations are done to show the surface temperature as a function of laser energy. This is shown in Fig. 6a. From extrapolating the data we conclude that the melting of the a-Si starts at approximately 100 mJ/cm^2.
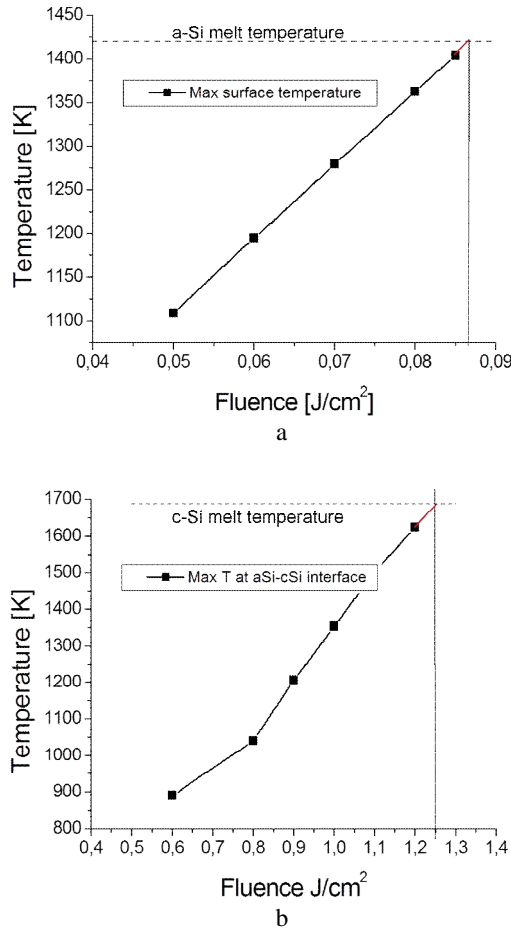
Fig. 6. Maximum temperature as a function of laser energy at (a) a-Si surface and (b) a-Si/c-Si interface.

Fig. 7. The temperature (a) and the phase (b) evolution of the structure, in the hole at different depths. Observe that the melt does not reach 1 μm depth. Laser pulse duration has been highlighted in gray. The legend is showing the x and y value of the monitored location, respectively.

More interesting feature can be found in the maximum temperature at the a-Si/c-Si interface as a function of laser energy. This is shown in Figure 6b. We define the onset of epitaxial growth to be when the a-Si/c-Si is molten. During several simulations, we monitor the temperature of this interface while increasing the laser energy. We observe that a successful epitaxial growth is realized with at least 1.4 J/cm^2 laser energy. With energies lower than this value, the c-Si interface will not melt and growth will then start from an amorphous seed. This laser energy is then used further to investigate the mechanism of epitaxial growth.
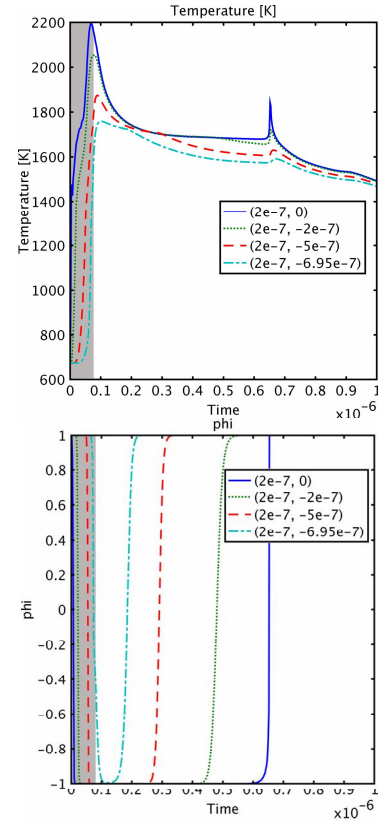
Fig. 7 shows the temperature and phase evolution of a-Si on top of the c-Si seed. The laser pulse duration has been indicated by a gray region in this figure. The phase value of 1 and -1 correspond to solid and liquid state, respectively. There is around 150 °C temperature increase at the onset of nucleation due to latent heat release. Figure 8 shows the moment of solidification for different points located 600 deep in the structure. There is a 40 ns time difference between two adjacent points at the same depth, 500 nm apart. This clearly shows that the growth front is not flat. The main argument that may be given in order to justify the formation of the secondary subgrains is the non-uniformity of the temperature resulting in non-flat growth front during the solidification. Fig. 7 shows that the temperature of the growth front is initially lower at the vicinity of SiO$_2$. In Fig. 4 two dotted lines are drawn at different depth of 400 and 600 nm, respectively. The temperature profiles across these two lines are shown in Fig. 9.
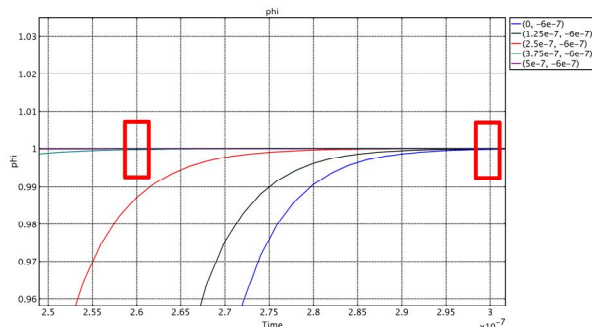
Fig. 8. This figure shows the solidification (phi becoming 1) moment of points at 600 nm depth. A time difference of 40 ns exists in the solidification onset between points (0,-600e-9) and (500e-9,-600e-9).
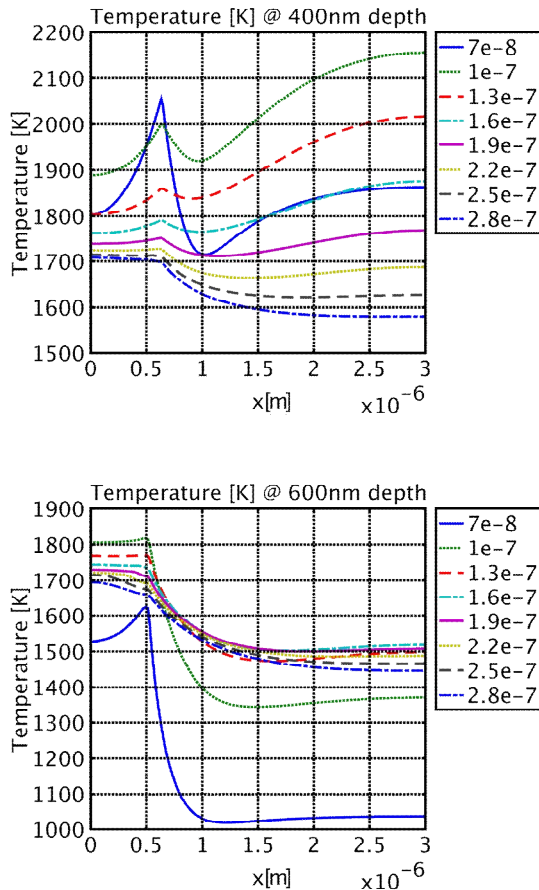

Fig. 9. Temperature profiles and its evolution of the structure at (a) 400 nm and (b) 600 nm depths from the surface. The legend is showing the time sweeps in seconds.

The following is observed:

• The closer we get to the heat sink, more the temperature gradient becomes. This is valid also in the oxide region.

• There is always an abrupt change of temperature at the Si/SiO_2 interface. This abruptness is reduced in magnitude at 400 nm depth. (Due to geometry curvature, the interface position is changed at different depth.)

• There is a delayed temperature profile in the oxide region. Since oxide has a lower thermal conductance, it becomes hot at a slower rate. Due to the same low thermal conductivity, it acts as a great heat insulator and stays hot even when silicon is solidified and cooler. Since this non-flat thermal gradient is a by-product of our specific process pattern, it is promising to optimize the structure to obtain the most lateral growth of silicon on top of this oxide.

Different temperature results in different solidification onset. Different onsets translates into different supercooling state just before solidification which will influence the melt front velocity. The location of the subgrains can be justified by this delayed solidification.

It is crucial to mention that in this simulation the nucleation model has been left out of consideration. This will influence the result since the temperature in some regions near the SiO_2 is below melting, while at the melt front it is much more above it. In a more realistic case, the silicon at some regions below the melt front should nucleate.

4. Summary

In the laser induced epitaxial growth of Si, facet formation at the SiO_2 sidewalls leads to formation of undesirable subgrains in the final crystallized films. These subgrains have a reproducible location at around the seeding hole. In order to understand the mechanism of the occurrence of these phenomena a simulation tool has been developed to clarify the mechanism of solidification.

The onset of epitaxial growth and its relation with laser energy have been confirmed. In case of lower energies the a-Si will not melt down to the c-Si interface. Phase-field simulation showed that the temperature of the growth front is not flat. This will cause a delayed solidification at the SiO_2 sidewall, causing the facet formation.

Acknowledgments

References

[1] J. C. Bean, H. J. Leamy, J. M. Poate, G. A. Rozgonyi, T. T. Sheng, J. S. Williams, and G. K. Celler, Appl. Phys. Lett., **33** 227 (1978).

[2] Paul Ch. van der Wilt, B. D. van Dijk, G. J. Bertens, R. Ishihara, and C. I. M. Beenakker, Appl. Phys. Lett., **79**, 1819 (2001).

[3] V. Rana, R. Ishihara, Y. Hiroshima, D. Abe, S. Inoue, T. Shimoda, W. Metselaar, C.I.M. Beenakker, IEEE Trans. on Elec. Dev., **52**, 12 (2005).

[4] H. Ming, Crystallographic Orientation- and Location-Controlled Si Single Grains on an Amorphous Substrate for Large Area Electronics, TU Delft, 2007, p. 52.

[5] D. T. J. Hurle, Journal of Crystal Growth, 147 (1995).

[6] A. Karma, W. J. Rappel, Phys. Rev. E, **57**, 4 (1998).

---

[*]Corresponding author: m.r.tajarimofrad@tudelft.nl